

## Physical modeling of thermal improvement in normally consolidated and overconsolidated soil

João Alberto Machado Leite<sup>1</sup> , Sérgio Tibana<sup>2#</sup> 

Article

### Keywords

Thermal consolidation  
Thermomechanics  
Undrained shear resistance

### Abstract

Knowledge of the soil-temperature relation and its peculiarities have been widely discussed in Geotechnics. Previous studies show that heated fine-grained soil induces pore pressure, and as a result, the soil exhibits a consolidation effect similar to that of conventional consolidation when pore pressure is dissipated. The outcome of this process depends on soil characteristics such as the overconsolidation ratio and plasticity. Consolidated soil typically induces positive pore pressure while overconsolidated one induces negative pore pressure when heated. The phenomenon described was explored in this study aimed at the thermal consolidation product regarding the decrease in void ratio and consequent increase in undrained shear strength ( $S_u$ ) of a soil submitted to heating. These aspects were investigated using physical models at 1g gravity field, built on a laboratory scale. The heat source was placed inside a driven torpedo pile model in a medium consisting of a kaolin and metakaolin mixture. The undrained shear strength profile was defined by T-Bar tests involving different effective stresses and consolidation temperatures. The results show that for both mediums (normally consolidated and overconsolidated), undrained shear strength tends to grow proportionally to the temperature variation and permanent volume change is reached after a heating-cooling cycle. On the other hand, undrained shear strength indicates less significant variations for higher overconsolidation ratios.

## 1. Introduction

The effect of temperature variation on soil properties has long been studied in geotechnics; however, the complex behavior of soils under temperature variation is a barrier to faster development and precise predictions in this area.

Some important applications have propelled geothermal studies, such as nuclear waste disposal (Slovic et al., 1991; Hueckel & Pellegrini, 1992; Delage et al., 2000) and, more recently, energy piles (Mimouni & Laloui, 2014; Chen & McCartney, 2016).

These studies include soil-pile interaction, soil and foundation thermal strains, ultimate pile capacity, and stress and strain development due to temperature variations (Ng et al., 2014, 2015; Murphy et al., 2015; Goode III & McCartney, 2015).

In addition to these practical studies, relevant contributions made by several researchers in theoretical and modeling contexts, such as Campanella & Mitchell (1968), Demars & Charles (1982), Baldi et al. (1988) and Delage et al. (2000), allow better understanding of temperature, physical and mechanical effects and indicate the possibility of thermal consolidation.

This thermal phenomenon is a consequence of clay heating that leads to greater expansion of the water in the system than the soil solid minerals. The expansion difference, combined with the low soil permeability, generates excess of pore pressure. The pore pressure dissipation induced by temperature changes and the consolidation of clays subjected to pressure changes occur in a similar manner (Campanella & Mitchell, 1968).

Normally consolidated soils tend to experience only contraction strains when heated and apparent pre-consolidation stress tends to increase. On the other hand, overconsolidated soils tend initially to experience a rise in volume at low temperatures, followed by contraction at high temperatures. This depends on soil characteristics and the overconsolidation ratio (OCR) (Plum & Esrig, 1969; Baldi et al., 1988; Cui et al., 2000; Laloui & Cekerevac, 2008).

Considering all these aspects, the State University of Norte Fluminense Darcy Ribeiro (UENF) research group has been investigating the effects of temperature change on the improvement of submarine clayey soil properties using physical modeling and special laboratory tests.

The main objective of this paper was to present the results of physical modeling 1g tests carried out at the

<sup>#</sup>Corresponding author. E-mail address: stibana@gmail.com

<sup>1</sup>Faculdade CNEC Rio das Ostras, Civil Engineering Laboratory, Rio das Ostras, RJ, Brazil.

<sup>2</sup>Universidade Estadual do Norte Fluminense Darcy Ribeiro, Civil Engineering Laboratory, Campos dos Goytacazes, RJ, Brazil.

Submitted on October 28, 2021; Final Acceptance on January 11, 2022; Discussion open until May 31, 2022.

<https://doi.org/10.28927/SR.2022.076421>



This is an Open Access article distributed under the terms of the Creative Commons Attribution License, which permits unrestricted use, distribution, and reproduction in any medium, provided the original work is properly cited.

UENF Geotechnical Centrifuge Laboratory. A number of undrained shear strength profiles obtained with T-Bar tests of the physical models were presented.

## 2. Materials and methods

### 2.1 Container and instrumentation

Four tests were carried out in a cylindrical container with inner diameter of 45.7 cm and height of 48 cm. A porous stone was placed at the bottom of the container to ensure double drainage and accelerate pore pressure dissipation during consolidation. Vertical load was applied to the top of the model with a perforated steel cap, where small holes allowed drainage from the top. The heat source was an electrical resistor installed inside a 25 cm-high torpedo pile model with an external diameter of 2.5 mm. The same beam used to place the torpedo pile model in the center of the container was used to install 2 rods in which the instrumentation was placed, as illustrated in Figure 1. The rods were positioned at 2 cm and 12 cm from the heat source and used to insert the pore pressure transducers and thermocouples into the model. Table 1 shows the distance and depth of each instrument associated with the rods. The consolidation system consisted of an electric motor coupled to a steel cap with outer diameter smaller than that of the inner container. The motor applied the load, which was recorded by a load cell.

### 2.2 Mixture of kaolin and metakaolin

A mixture of kaolin (40%) and metakaolin (60%) by weight was prepared with an initial moisture content of  $1.5 \times$  liquid limit to be used in the model. Table 2 summarizes the results of the physical properties of the mud. The results presented show that the mixture was a fine mud containing 84.2% silt and clay, and the specific gravity of particles was

2.63. The liquid and plastic limits were 62.5 and 35.7%, respectively. The mixture was prepared in a mixer adapted to apply vacuum during the 30-minute homogenization process.

### 2.2.1 Model preparation

The homogenized and de-aerated mud was poured into the container and the load application system was installed to consolidate it in tests with overconsolidated models. The normally consolidated model was subjected to its self-weight consolidation.

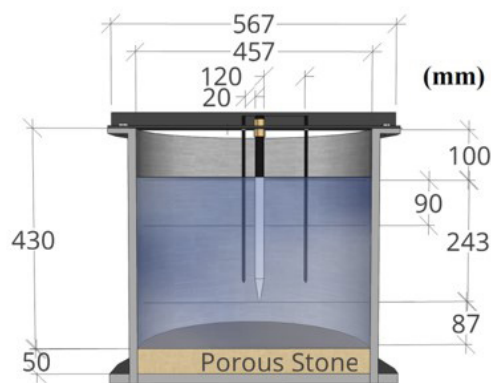
Three overconsolidated models were prepared, each with final vertical effective stress application of 25, 50 and 100 kPa. Given that at the end of consolidation the effective soil height was insufficient to install the instrumentation and carry out the tests, another layer of sludge was consolidated with the same vertical effective stress. Thus, the steel cap was removed and the instrumentation and torpedo pile were installed.

### 2.3 Thermal consolidation and undrained shear strength ( $S_u$ )

The thermal consolidation of each model was carried out with temperature increases of 30 and 60 °C above ambient

**Table 1.** Instrument configuration in the containers.

Radial distance from pile (mm)	Depth inside soil (mm)	Thermocouple	PP Transducer
20	45	H11	PP11
	90	H12	PP12
	135	H13	-
120	45	H21	PP21
	90	H22	PP22
	135	H23	-



(a)



(b)

**Figure 1.** (a) lay-out of the container and instrumentation (b) torpedo and instrumentation installation.

**Table 2.** Characterization of the kaolin and metakaolin mixture.

	Fine sand (%)	Silt (%)	Clay (%)	G	LL (%)	PL (%)	PI (%)
Mixture	15.7	58.8	25.4	2.63	62.5	35.7	26.7

**Table 3.** T-bar test details for each stage.

Applied stress (kPa)	Thermal load	Radial distance from the pile (cm)			
		2	5	8	12
0	$\Delta T$ 30 °C		X		X
	$\Delta T$ 60 °C		X		X
	$\Delta T$ 0 °C		X		X
25	$\Delta T$ 30 °C				
	$\Delta T$ 60 °C	X	X	X	X
	$\Delta T$ 0 °C	X	X	X	X
50	$\Delta T$ 30 °C		X	X	X
	$\Delta T$ 60 °C		X	X	X
	$\Delta T$ 0 °C		X	X	X
100	$\Delta T$ 30 °C		X	X	
	$\Delta T$ 60 °C	X	X	X	
	$\Delta T$ 0 °C	X	X	X	

temperature (25 °C). The temperature of the model was increased by turning on the heater. The increase and dissipation of excess pore pressure was monitored by pore pressure transducers. Thus, during each temperature increment and after the heater was turned off and the model cooled, the undrained shear strength profile was determined at different distances from the pile.

The undrained shear strength profiles of all tests were determined from the mini T-Bar tests. The T-Bar tests were conducted according to Stewart & Randolph (1991). Prior to the thermal consolidation of all the models, a T-bar test was carried out to obtain the initial undrained shear strength profile of each model. These results were used to calculate the  $S_u$  gain after thermal consolidation.

A summary of test configurations is presented in Table 3 and Figure 2. Table 3 shows the temperature variations applied ( $\Delta T=30$  °C,  $\Delta T=60$  °C and  $\Delta T=0$  °C) and the distances from the pile where the tests were performed (2, 5, 8 and 12 cm). Each of these tests was compared to the initial reference test, carried out prior to thermal consolidation. Figure 2 illustrates the arrangement and distribution of the tests performed in each heating step as an example of the pattern used for all models.

### 3. Results and discussions

#### 3.1 Mechanical consolidation

The mechanical consolidation of each container was carried out in steps until the final effective stress was reached. The mechanical consolidation curves of the models are presented

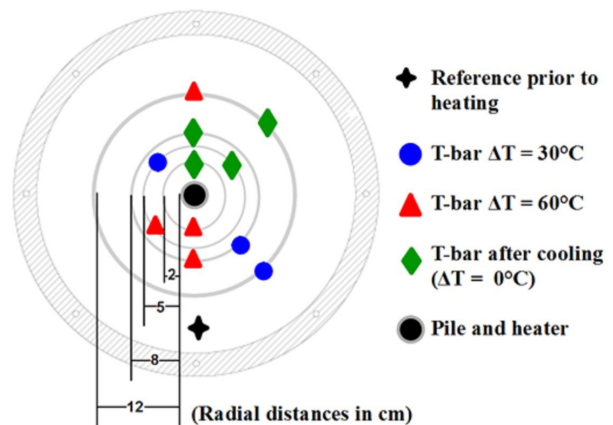


**Figure 2.** Generic T-bar test arrangement showing the number and position of tests conducted for each heating step.

in Figure 3, while Table 4 shows the void ratio development for each stress step of the consolidation. Given the good agreement of the curves, it can be considered that the methodology produced very similar models, suggesting that the undrained shear strength obtained with the T-Bar in each model can be compared. After mechanical consolidation, the steel cap was removed and the torpedo pile with the heater and instrumentation rods installed.

#### 3.2 Thermal consolidation

Figure 4 demonstrates the evolution of temperature over time, showing the temperature of the thermocouples on the surface of the pile, such as those placed at different depths

**Table 4.** Void ratio variation during mechanical consolidation for different stresses applied to each container.

Total Applied Stress (kPa)	0.00 kPa	2.50 kPa	5.00 kPa	10.00 kPa	25.00 kPa	50.00 kPa	100.00 kPa
0.00	2.48	-	-	-	-	-	-
25.00	2.53	2.24	1.96	1.77	1.61	-	-
50.00	2.47	2.22	2.02	1.70	1.56	1.53	-
100.00	2.46	2.18	2.02	1.78	1.60	1.52	1.40

and distances from the pile, according to Table 1. All the tests started with a T-bar test before any temperature was applied in the model. Next, an increase of 30 °C above room temperature was applied to the heater inside the pile, corresponding to time zero in Figure 4. The temperature of the pile rapidly rose to about 55 °C, as did the soil temperature, increasing more for lower positions in the soil and for distances nearer the heat source, as shown in the curves. After 24 h, the temperature in the system stabilized, and a series of T-bar tests were conducted. A new 30 °C rise was then applied to the heater, reaching a total variation of about 60 °C above ambient temperature. Once again, after 24 h, another series of T-bar tests were carried out, the heater was turned off and the system started to cool down naturally. Finally, after the system had cooled completely, identified by the equalization of all the thermocouples with the ambient temperature, the last series of T-bar tests were performed. This process was followed for all the containers, each with a different stress state.

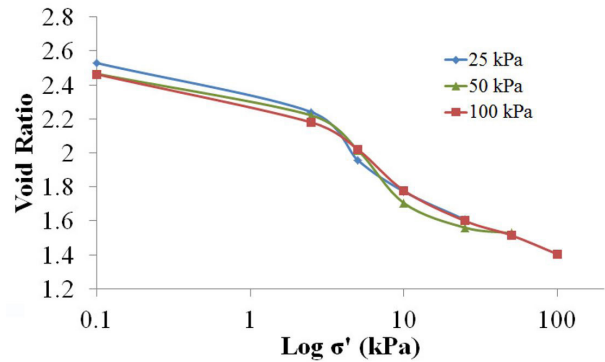
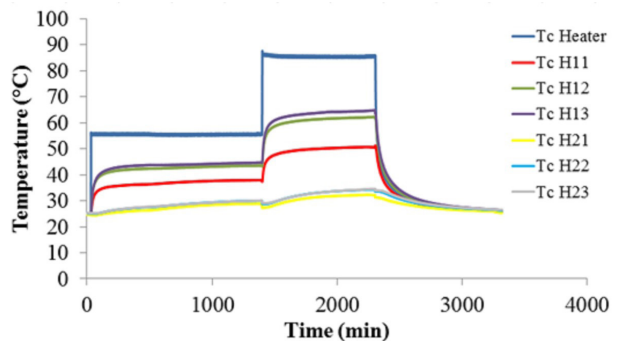
### 3.3 T-Bar tests

The results showed a close relation between temperature and  $S_u$  for clays, where temperature invariably influenced soil response. In normally consolidated tests, which obtained the lowest stress levels,  $S_u$  strength gain during and after heating was the most noticeable, especially in the tests conducted during temperature variations. Despite the low  $S_u$  magnitude variations in absolute values, they were the most relevant, proportionally to their initial strength.

Overconsolidated soil also showed undrained shear strength variations. In these cases, the noteworthy pattern observed among the different containers consisted of increased strength in the final profile portions, at the greatest soil depths.

This region experienced positive  $S_u$  variations for the different overconsolidation levels in the containers and the different distances tested. It is believed that these patterns are a consequence of two common characteristics in the region analyzed: the proximity to the bottom container drainage and the consequence of a more lightly overconsolidated zone at the greatest depths.

In addition, despite exhibiting greater average magnitude variation, the average strength increase for higher overconsolidation levels revealed a smaller percentage variation compared to the initial (reference) strength when compared to the soils with lower overconsolidation levels.

**Figure 3.** Consolidation curves of the overconsolidated models.**Figure 4.** Temperature development over time on thermocouples inserted into the models.

These findings can be better visualized in the following bar graphs (Figures 5 to 8), which compare, among the different consolidation levels, (a) the absolute value of the average  $S_u$  variation, and (b) the average  $S_u$  variation percentage, for each thermal load applied ( $\Delta T=30$  °C and  $\Delta T=60$  °C) and for the end of the heating-cooling cycle ( $\Delta T=0$  °C). Figures 5, 6, 7 and 8 show the relationships described for distances from the pile surface of 2, 5, 8 and 12 cm, respectively.

An example of the interpretations reported can be extracted from the tests carried out at a distance of 2 cm for containers subjected to 25 and a 100 kPa during consolidation, as shown in Figure 5. For the former, the absolute average  $S_u$  increments in the studied region were 7.32 and 1.05 kPa during  $\Delta T=60$  °C and after system cooling,

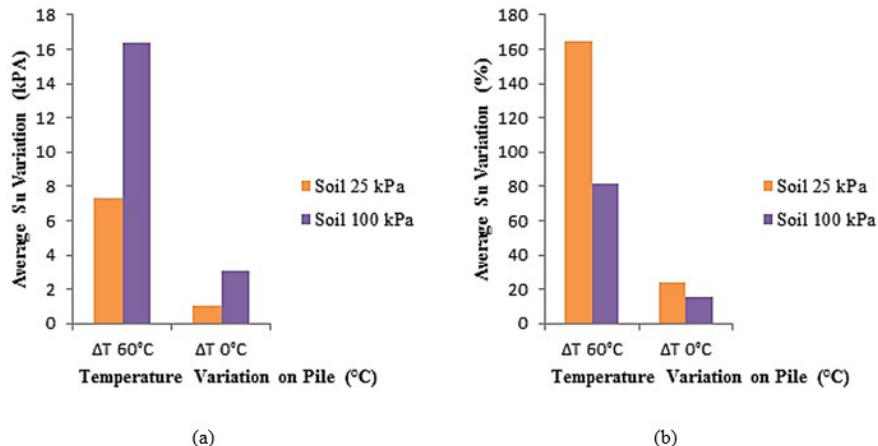


Figure 5. Average  $S_u$  variation in (a) absolute values and (b) percentage for the 2 cm test distance.

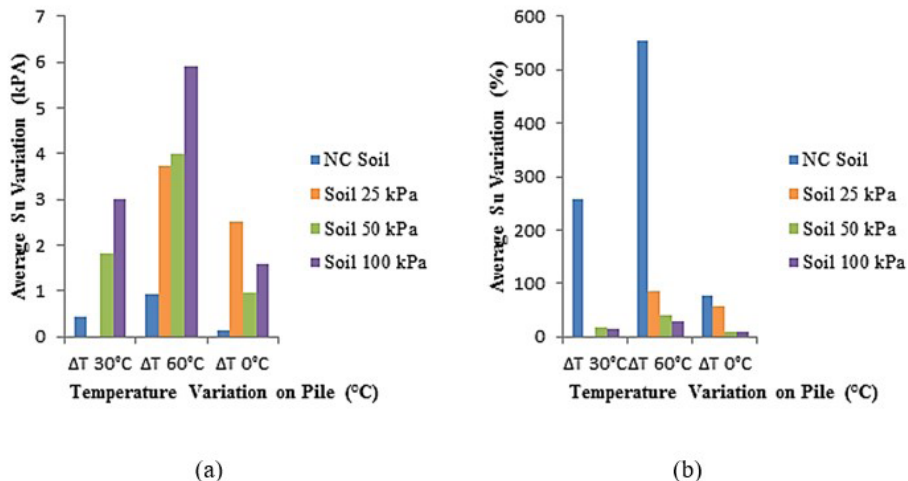


Figure 6. Average  $S_u$  variation in (a) absolute values and (b) percentage for the 5 cm test distance.

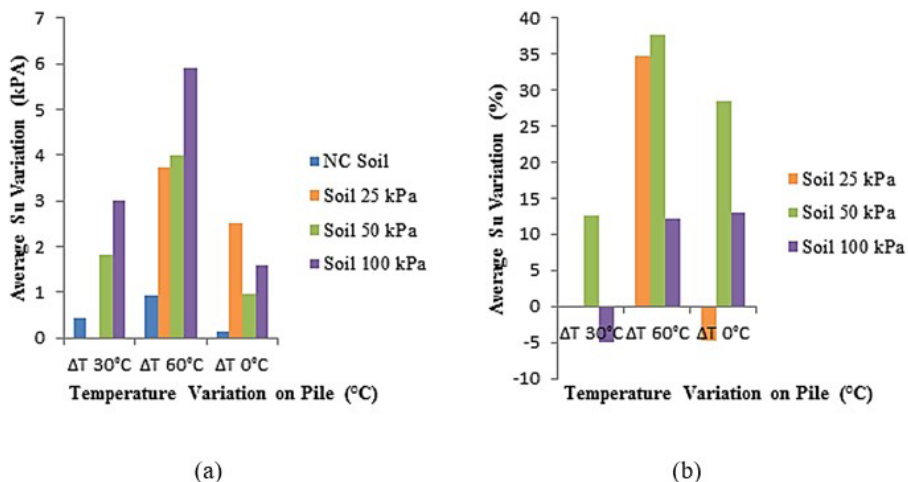


Figure 7. Average  $S_u$  average in (a) absolute values and (b) percentage for the 8 cm tests distance.

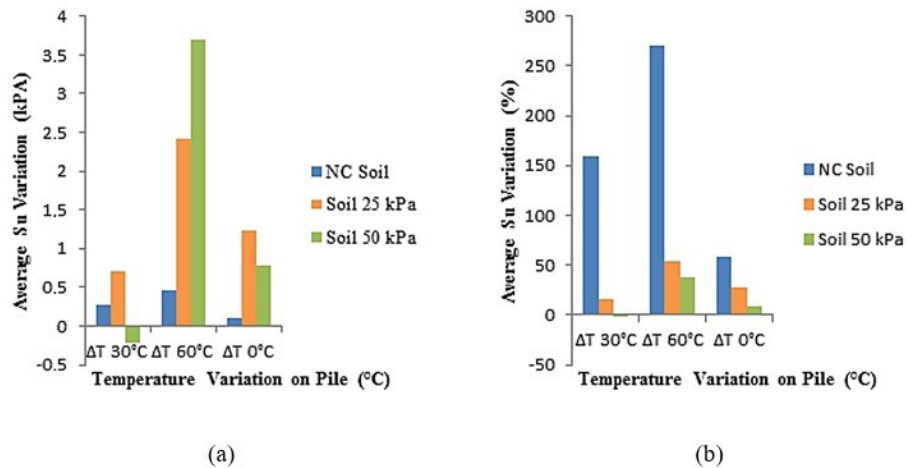


Figure 8. Average  $S_u$  variation in (a) absolute values and (b) percentage for the 12 cm test distance.

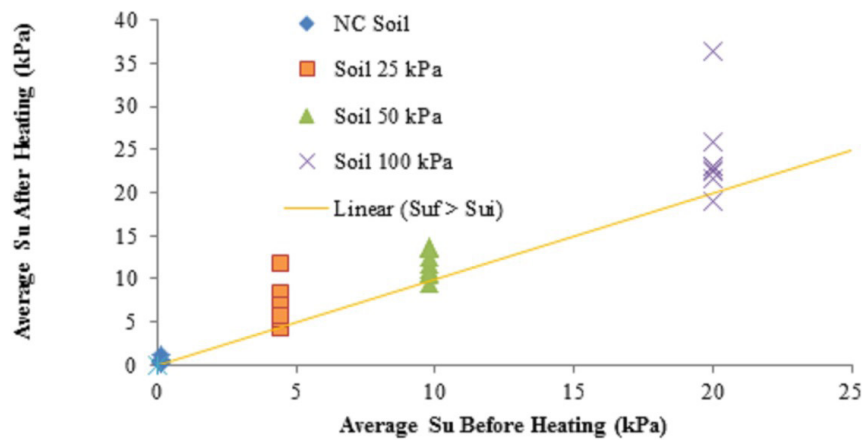


Figure 9. Relation between the average strength of tests under the influence of temperature and the initial average strength prior to heating for different consolidation levels.

respectively, while the average percentage increase for the same situations were 165 and 24%. For the latter container, the absolute average  $S_u$  increments were 16.28 and 3.1 kPa, during  $\Delta T=60^\circ\text{C}$  and  $\Delta T=0^\circ\text{C}$ , while the average gains were 82 and 15%.

The graphs show that the highest average  $S_u$  variation occurred during heating with a  $60^\circ\text{C}$  variation on the pile. Moreover, there was relevant  $S_u$  variation even for the furthest distance – 12 cm from the pile surface. Finally, it is important to note that some tests showed negative average strength variation.

A summary of the influence of temperature on the average undrained shear strength of the soils is illustrated in Figure 9. In the figure, all the average  $S_u$  variation values are plotted as a function of their initial reference value, prior to heating, for each consolidation level. On the graph, a  $45^\circ$  slope line divides the points with strength gain due to the influence of temperature – those above the line, and with strength loss – those below the line.

## 4. Conclusions

In general, it can be said that the experimental program achieved the initial goals. Mechanical and thermal consolidation worked very well. The T-Bar tests made it possible to determine the undrained shear strength profiles of the models in the different stages.

Due to the low level of effective stress at  $1g$ , an average undrained shear strength profile was determined, and the efficiency of thermal consolidation evaluated by comparing the average value of each stage against the initial value.

As expected, the normally consolidated and slightly overconsolidated models showed the greatest percentage  $S_u$  increase, while the strongly overconsolidated models show that thermal consolidation is less efficient. In addition, results after the heating-cooling cycle reveal some irreversible changes, which is more interesting from a technical standpoint.

## Acknowledgements

The authors would like to thank Petrobras for the financial support for this research project. The work described in this article is part of a Term of Cooperation signed between Petrobras and the State University of Northern Fluminense Darcy Ribeiro (UENF), to develop the research project entitled “Optimized Solutions of Fixed Anchorage Points” (Contractual Instrument 0050.0098204.15.9). The first author is grateful to the UENF for the scholarship granted.

## Declaration of interest

The authors have no conflicts of interest to declare. All co-authors have observed and affirmed the contents of the paper and there is no financial interest to report.

## Authors' contributions

João Alberto Machado Leite: conceptualization, Data curation, Writing – original draft. Sérgio Tibana: conceptualization, Methodology, Supervision, Project administration, Writing – review & editing.

## List of symbols

%	percentage;
°C	degrees Celsius;
cm	centimeters;
g	acceleration of gravity;
h	hours;
kPa	kiloPascal;
LL	liquid limit;
mm	millimeters;
NC	normally consolidated;
OCR	over consolidation ratio;
Su	undrained shear strength;
UENF	Universidade Estadual do Norte Fluminense
$\Delta T$	temperature variation;
$\sigma$	effective stress.

## References

- Baldi, G., Hueckel, T., & Pellegrini, R. (1988). Thermal volume changes of the mineral-water system in low-porosity clay soils. *Canadian Geotechnical Journal*, 25(4), 807-825. <http://dx.doi.org/10.1139/t88-089>.
- Campanella, R.G., & Mitchell, J.K. (1968). Influence of temperature variations on soil behavior. *Journal of the Soil Mechanics and Foundation Engineering Division*, 94(3), 709-734. <http://dx.doi.org/10.1061/JSFEAQ.0001136>.
- Chen, D., & McCartney, J.S. (2016). Parameters for load transfer analysis of energy pile in uniform nonplastic soils. *International Journal of Geomechanics*, 17(7), 1-17. [http://dx.doi.org/10.1061/\(ASCE\)GM.1943-5622.0000873](http://dx.doi.org/10.1061/(ASCE)GM.1943-5622.0000873).
- Cui, Y.J., Sultan, N., & Delage, P. (2000). A thermomechanical model for saturated clays. *Canadian Geotechnical Journal*, 37(3), 607-620. <http://dx.doi.org/10.1139/t99-111>.
- Delage, P., Sultan, N., & Cui, Y.J. (2000). On the thermal consolidation of Boom clay. *Canadian Geotechnical Journal*, 37(2), 343-354. <http://dx.doi.org/10.1139/t99-105>.
- Demars, K.R., & Charles, R.D. (1982). Soil volume changes induced by temperature cycling. *Canadian Geotechnical Journal*, 19(2), 188-194. <http://dx.doi.org/10.1139/t82-021>.
- Goode III, J.C., & McCartney, J.S. (2015). Centrifuge modeling of boundary restraint effects in energy foundations. *Journal of Geotechnical and Geoenvironmental Engineering*, 141(8), 04015034. [http://dx.doi.org/10.1061/\(ASCE\)GT.1943-5606.0001333](http://dx.doi.org/10.1061/(ASCE)GT.1943-5606.0001333).
- Hueckel, T., & Pellegrini, R. (1992). Effective stress and water pressure in saturated clays during heating-cooling cycles. *Canadian Geotechnical Journal*, 29(6), 1095-1102. <http://dx.doi.org/10.1139/t92-126>.
- Laloui, L., & Cekerevac, C. (2008). Non-isothermal plasticity model for cyclic behaviour of soils. *International Journal for Numerical and Analytical Methods in Geomechanics*, 32(5), 437-460. <http://dx.doi.org/10.1002/nag.629>.
- Mimouni, T., & Laloui, L. (2014). Towards a secure basis for the design of geothermal piles. *Acta Geotechnica*, 9(3), 355-366. <http://dx.doi.org/10.1007/s11440-013-0245-4>.
- Murphy, K.D., McCartney, J.S., & Henry, K.S. (2015). Evaluation of thermo-mechanical and thermal behavior of full-scale energy foundations. *Acta Geotechnica*, 10(2), 179-195. <http://dx.doi.org/10.1007/s11440-013-0298-4>.
- Ng, C.W.W., Shi, C., Gunawan, A., & Laloui, L. (2014). Centrifuge modelling of energy piles subjected to heating and cooling cycles in clay. *Geotechnique Letters*, 4(4), 310-316. <http://dx.doi.org/10.1680/geolett.14.00063>.
- Ng, C.W.W., Shi, C., Gunawan, A., Laloui, L., & Liu, H.L. (2015). Centrifuge modelling of heating effects on energy pile performance in saturated sand. *Canadian Geotechnical Journal*, 52(8), 1045-1057. <http://dx.doi.org/10.1139/cgj-2014-0301>.
- Plum, R.L., & Esrig, M.I. (1969). *Some temperature effects on soil compressibility and pore water pressure* (pp. 231-242). Washington: Highway Research Board.
- Slovic, P., Flynn, J., & Layman, M. (1991). Perceived risk, trust, and the politics of nuclear waste. *Science*, 254(5038), 1603-1607. <http://dx.doi.org/10.1126/science.254.5038.1603>.
- Stewart, D.P., & Randolph, M.F. (1991). A new site investigation tool for the centrifuge. In *Proc. International Conference on Centrifuge Modelling – Centrifuge* (pp. 531-538), Boulder.